



HHS Public Access

Author manuscript

JAMA Ophthalmol. Author manuscript; available in PMC 2018 June 22.

Published in final edited form as:

JAMA Ophthalmol. 2016 November 01; 134(11): 1272–1280. doi:10.1001/jamaophthalmol.2016.3519.

Histopathological Insights Into Choroidal Vascular Loss in Clinically Documented Cases of Age-Related Macular Degeneration

Johanna M. Seddon, MD, ScM,

Ophthalmic Epidemiology and Genetics Service, New England Eye Center, Tufts Medical Center, Boston, Massachusetts; Department of Ophthalmology, Tufts University School of Medicine, Boston, Massachusetts; Sackler School of Graduate Biomedical Sciences, Tufts University, Boston, Massachusetts

D. Scott McLeod,

Department of Ophthalmology, Wilmer Ophthalmological Institute, Johns Hopkins Hospital, Baltimore, Maryland

Imran A. Bhutto, MD, PhD,

Department of Ophthalmology, Wilmer Ophthalmological Institute, Johns Hopkins Hospital, Baltimore, Maryland

Mercedes B. Villalonga, BA,

Ophthalmic Epidemiology and Genetics Service, New England Eye Center, Tufts Medical Center, Boston, Massachusetts

Rachel E. Silver, MPH,

Ophthalmic Epidemiology and Genetics Service, New England Eye Center, Tufts Medical Center, Boston, Massachusetts

Adam S. Wenick, MD, PhD,

Department of Ophthalmology, Wilmer Ophthalmological Institute, Johns Hopkins Hospital, Baltimore, Maryland

Malia M. Edwards, PhD, and

Department of Ophthalmology, Wilmer Ophthalmological Institute, Johns Hopkins Hospital, Baltimore, Maryland

Corresponding Author: Gerard A. Luty, MS, PhD, Wilmer Ophthalmological Institute, M041 Smith Bldg, Johns Hopkins Hospital, 400 N Broadway, Baltimore, MD 21287-9115 (gluty@jhmi.edu).

Author Contributions: Drs Seddon and Luty had full access to all the data in the study and take responsibility for the integrity of the data and the accuracy of the data analysis. Drs Seddon and McLeod contributed equally to the manuscript. *Concept and design:* Seddon, Wenick, Luty. *Acquisition, analysis, or interpretation of data:* All Authors.

Drafting of the manuscript: Seddon, McLeod, Villalonga, Silver, Luty.

Critical revision of the manuscript for important intellectual content: All Authors.

Statistical analysis: McLeod, Bhutto, Edwards. *Obtaining funding:* Seddon, Luty. *Administrative, technical, or material support:* Seddon, Bhutto, Villalonga, Silver, Edwards, Luty. *Study supervision:* Seddon, Villalonga, Silver, Luty.

Conflict of Interest Disclosures: All authors have completed and submitted the ICMJE Form for Disclosure of Potential Conflicts of Interest and none were reported.

Additional Contributions: We thank our participating eye donors and their families.

Gerard A. Luty, MS, PhD

Department of Ophthalmology, Wilmer Ophthalmological Institute, Johns Hopkins Hospital, Baltimore, Maryland

Abstract

IMPORTANCE—Age-related macular degeneration (AMD) is a multifactorial disease with genetic and environmental factors contributing to risk. Histopathologic changes underlying AMD are not fully understood, particularly the relationship between choriocapillaris (CC) dysfunction and phenotypic variability of this disease.

OBJECTIVE—To examine histopathologic changes in the CC of eyes with clinically documented AMD.

DESIGN, SETTING, AND PARTICIPANTS—The study was designed in 2011. Tissues were collected post mortem (2012-2016), and histopathological images were obtained from participants enrolled in AMD studies since 1988. Clinical records and images were collected from participants as standard protocol. Eyes without AMD (n = 4) and eyes with early (n = 9), intermediate (n = 5), and advanced stages of AMD (geographic atrophy, n = 5; neovascular disease, n = 13) were evaluated. Choroidal vasculature was labeled using Ulex europaeus agglutinin lectin and examined using confocal microscopy.

MAIN OUTCOMES AND MEASURES—A standardized classification system was applied to determine AMD stage. Ocular records and images were reviewed and histopathologic analyses performed. Viability of the choroidal vasculature was analyzed for each AMD stage.

RESULTS—All participants were white. Fourteen were male, and 16 were female. The mean age was 90.5 years among AMD patients and 88.5 years among control participants. Submacular CC dropout without retinal pigment epithelial (RPE) loss was observed in all cases with early stages of AMD. Higher vascular area loss for each AMD stage was observed compared with control participants: 20.5% in early AMD (95% CI, 11.2%-40.2%; $P < .001$), 12.5% in intermediate AMD (95% CI, 2.9%-21.4%; $P = .01$), 39.0% loss in GA (95% CI, 32.1%-45.4%; $P < .001$), and 38.2% loss in neovascular disease where RPE remained intact (95% CI, 27.7%-47.9%; $P < .001$). Hypercellular, apparent neovascular buds were adjacent to areas of CC loss in 22.2% of eyes with early AMD and 40% of eyes with intermediate AMD.

CONCLUSIONS AND RELEVANCE—Retinal pigment epithelial atrophy preceded CC loss in geographic atrophy, but CC loss occurred in the absence of RPE atrophy in 2 of 9 eyes with early-stage AMD. Given the cross-sectional nature of this study and the small number of eyes evaluated, definitive conclusions regarding this progression cannot be determined with certainty. We speculate that neovascular buds may be a precursor to neovascular disease. Hypoxic RPE resulting from reduced blood supply might upregulate production of vascular endothelial growth factor, providing the stimulus for neovascular disease.

Age-related macular degeneration (AMD) is a chronic and degenerative disease affecting the central part of the retina. It is the leading cause of irreversible visual loss in adults older than 60 years.^{1,2} The etiology of AMD is multifactorial, and contributions of both genetic and environmental risk factors are well established²⁻⁴; however, histopathologic changes

underlying this disease are not fully understood. To our knowledge, the relationship between choriocapillaris (CC) loss and AMD severity has not been determined.

The pathology of AMD is characterized by the degeneration of photoreceptors and retinal pigment epithelium (RPE), deposits between the RPE and Bruch membrane, and CC loss. There is much debate regarding the sequence of cellular degeneration in AMD, particularly in the advanced forms of neovascular disease (NV) and geographic atrophy (GA). These subtypes are generally preceded by early and intermediate stages characterized by drusen formation and pigmentary abnormalities (defined as hypopigmentation or hyperpigmentation of the RPE). Choriocapillaris and RPE loss have been documented in both GA and NV, although the mechanism by which the cellular degeneration proceeds may differ for each subtype.⁵⁻⁸

To develop new preventative and therapeutic strategies, it is essential to understand the interplay of modifiable and genetic risk factors in conjunction with the underlying structural changes in AMD. The CC is vital for the survival of photoreceptors and RPE, and this study provides unique insights into AMD-associated CC changes. Our research evaluates the relationship between CC loss and the phenotypic appearance of the eye using documented ocular histories and fundus photography from patients with all stages of AMD.

Methods

Donor Eyes

Eyes were acquired post mortem by the Ophthalmic Epidemiology and Genetics Service, New England Eye Center, Tufts Medical Center, Boston, Massachusetts. Participants were previously enrolled in studies of AMD. This research adhered to the tenets of the Declaration of Helsinki and was approved by institutional review boards at Tufts Medical Center and Johns Hopkins School of Medicine. Written informed consent was obtained. Mean time elapsed between death and enucleation was 10 hours. Thirty-two eyes from participants clinically diagnosed as having AMD (mean age, 90.5 years) and 4 eyes from control individuals without AMD (mean age, 88.5 years) were evaluated. All donors were white.

Clinical ocular records and images were obtained prior to death as part of ongoing AMD studies beginning in 1988. Eyes were classified prior to death by masked readers based on ocular examination and fundus photography using the Clinical Age-Related Maculopathy Staging system.⁹ Grades were defined as follows: grade 1, no AMD (no drusen or a few small drusen <63 μ m); grade 2, early AMD, with 3 distinct subtypes: grade 2A (several small drusen or <15 intermediate drusen 63-124 μ m, no RPE abnormalities), grade 2B (no drusen, RPE abnormalities), and grade 2C (drusen and RPE abnormalities); grade 3, intermediate AMD with 2 subtypes: grade 3A (several intermediate drusen or any large drusen) and grade 3B (several intermediate drusen or any large drusen with drusenoid RPE detachment); grade 4 (central and noncentral GA); and grade 5 (NV with choroidal neovascularization [CNV]). The mean time elapsed from last clinical examination to death was 14.3 months. Postmortem observation of the macula was performed during gross

examination by a masked observer using transmitted and reflected illumination with a dissecting microscope (Stemi 2000; Carl Zeiss Meditec Inc).

Tissue Preparation

Globes were opened at the limbus, anterior segments were removed, and posterior eyecups were imaged using a QImaging MicroPublisher 5.0 Real-Time Viewing camera on a Zeiss STEMI 2000 microscope. Vitreous was removed and retinas were excised for use in other studies.¹⁰ The presence of a complete sheet of RPE was determined in observations and photographs of the eyecup without retina. The RPE was removed with EDTA as previously described. Additional images of choroids were captured without RPE. Retinal pigment epithelium–denuded choroids were dissected from the sclera and washed in 0.1M cacodylate at 4°C and fixed in 2% paraformaldehyde in 0.1M cacodylate buffer at 4°C overnight for whole-mount immunohistochemistry.

Whole-Mount Immunohistochemistry

Choroids were washed in Tris-buffered saline with 0.1% Triton X-100 and incubated with fluorescein isothiocyanate conjugated to Ulex europaeus agglutinin lectin (UEA; Sigma L9006; 1:100) for 48 hours at 4°C. Immunofluorescence in flat mounts was imaged with a confocal microscope (710; Carl Zeiss MicroImaging) at 488-nm excitation.

Morphometric Analysis

Maximum intensity projection 5× stitched images of sub macular choroid were exported from Zen Software as full-resolution TIFF images. Three 1204×1204 pixel dimension selections (equivalent to 1 mm²) were made of regions in submacula and pasted into new image documents. These images were then imported into Image J software (Image J, US National Institutes of Health). For CC diameters, the scale was set in the analyze menu and 10 lumenal diameter measurements were made on randomly selected capillary segments that were not at bifurcations in each calibrated image (30 measurements total). For percent vascular area determinations (%VA), thresholding was performed and images were converted to binary (black vessels on a white background). Measurements were made using the “compute percent black and white” command in the measurement macros.

Data are reported as mean (SD). Mean CC diameter and %VA loss in early AMD, intermediate AMD, and the 2 advanced subtypes were compared with aged control individuals using a *t* test with unequal variances assumed, and 95% confidence intervals were calculated.

Results

Ulex europaeus agglutinin has been used previously to label viable choroidal blood vessels in cross sections.¹¹ Incubation of whole human choroids with UEA–fluorescein isothiocyanate resulted in succinct fluorescent staining of the choroidal vasculature. The eTable in the Supplement summarizes the clinical and histopathological characteristics of donor eyes (n = 36) from 30 patients. A representative eye at each grade is presented in the figures.

Grade 1

Control eyes (n = 4) had no characteristics of AMD. In some cases, a few small drusen were observed. Figure 1 A-C shows fundus and gross images for patient 3 (eTable in the Supplement). This woman was followed up for 13 years with no history of AMD. Baseline visual acuity was 20/25 and declined to 20/70, likely owing to cataract reported at her last visit prior to death.

Choroidal flat mounts stained with UEA at low and high magnification are shown (Figure 1D-F). Ulex europaeus agglutinin staining of choroidal vasculature was robust, illustrating the normal high density of CC (mean [SD], 77.8% [3.5%] VA in submacula); however, the deep large vessels in the Haller layer were less intensely labeled in some patients, presumably owing to a lack of lectin penetration into choroidal stroma. The typical homogeneous, freely interconnecting pattern of CC with broad-diameter lumens (mean [SD] CC diameter, 12.8 [1.2] μm) was present in the submacular region (Figure 1F). Few degenerative capillary segments (UEA⁻) were present.

Grade 2A

Eyes with early AMD had small or few intermediate drusen without RPE abnormalities (n = 5). A representative grade 2A eye is shown in eFigure 1 in the Supplement. This female participant (patient 7, eTable in the Supplement) was followed up for 2 years with clinical signs of early AMD (eFigure 1A-C in the Supplement). Her visual acuity remained stable (baseline, 20/30; final, 20/40).

Ulex europaeus agglutinin staining demonstrated sub-macular capillary segment loss (eFigure 1D in the Supplement, mean [SD], 59.3% [5.8%] VA in submacula vs 81.1% [7.5%] VA in perimacular region) in the presence of an intact RPE monolayer. Higher magnification of the submacular CC demonstrated loss in interconnecting capillary segments, resulting in gaps in the normally dense capillary network (eFigure 1E in the Supplement). Presumed neovascular buds were also observed adjacent to the area of CC loss. The CC appeared normal outside the submacular region (eFigure 1F in the Supplement, mean [SD] CC diameter, 13.2 [0.4] μm in submacula vs 18.0 [1.1] μm in perimacular region).

Grade 2C

Eyes graded 2C had small or intermediate drusen with RPE abnormalities (n = 4). A representative eye is shown in Figure 2 (patient 10, eTable in the Supplement). This female patient was graded 2A (visual acuity 20/20) at age 73 years and was followed up for 11 years. At her final visit 3 years prior to death, she was graded 2C with 20/30 visual acuity.

This patient's baseline fundus photograph is shown in Figure 2A, and the postmortem gross photograph (Figure 2B) reveals the pigmentary abnormalities associated with grade 2C. After removing the retina, drusen are seen in the image taken before removal of the RPE (Figure 2B). Ulex europaeus agglutinin staining demonstrated a large area of submacular CC loss (Figure 2C) that was apparent at higher magnification (Figure 2D). The CC appeared normal in the perimacular region (Figure 2E, mean [SD], 43% [8.7%] VA in the submacula

vs 76% [2.8%] in the perimacular region). The mean (SD) submacular CC diameter was 13.5 (0.7) μm vs 17.4 (1.8) μm in the perimacular region. At higher magnification, there were areas of intense UEA staining in the sub-macular choroid near the border of CC loss that appeared to represent hyperplastic endothelial cells and apparent neovascular buds that were present in 22.2% of the eyes with early AMD (Figure 2F).

Grade 3

A representative grade 3 eye (patient 13, eTable in the Supplement) is shown in Figure 3 (n = 5). This patient was followed up for 17 years, progressing from grade 2A to 3A. He exhibited large, confluent drusen in the left eye, the distinctive feature of intermediate AMD, at his final visit 3 months prior to death. His visual acuity declined from 20/20 to 20/70 during follow-up.

Many large drusen were apparent in the infrared and spectral-domain optical coherence tomographic (OCT) images (Figure 3A and B). The low-magnification image of UEA-stained choroid demonstrates substantial CC dropout in the submacula and other areas (Figure 3C). The mean (SD) % VA in submacula was 13.5% less than control participants (54.3% [2.5%]), although capillary diameters were normal (14 [1.2] μm). An area temporal to macula had CC loss adjacent to an anomalous vascular formation (higher magnification, Figure 3D), near drusen shown with spectral-domain OCT (Figure 3B). Figure 3E-G displays slices from the z-stack of this formation, demonstrating that it is above CC (Figure 3E) and has multiple connections to the choroidal vasculature (arrowheads, Figure 3G). These apparent neovascular buds were observed in 40% of grade 3 eyes.

Grade 4

Patients with GA had a sharply demarcated area of RPE atrophy, often accompanied by an adjacent field of drusen (n = 5). The submacular CC in patients with GA had severely attenuated vas-culature in the area of RPE atrophy. A representative eye (patient 15, eTable in the Supplement) is shown in Figure 4. This patient presented with intermediate AMD and developed GA 4 years later with visual decline from 20/60 to counting fingers.

A field of drusen temporal to the area of RPE atrophy is apparent in the fundus photograph and the gross photo graph prior to removing RPE (Figure 4A and B). Many of the drusen were lost after incubation with EDTA, suggesting they may have been calcific because EDTA is a calcium chelator (Figure 4C). At higher magnification, CC attenuation is apparent under and around drusen and is associated with RPE loss (eFigure 2 in the Supplement). In the center of the area of RPE atrophy, there was an approximately 50% loss of vasculature in submacular choroid (Figure 4E). The mean (SD) % VA was 38.3% (5%) in the submacular area of RPE atrophy compared with 81.9% (23.9%) outside the area of RPE atrophy. The remaining capillaries in the atrophic region were highly constricted compared with aged control sub-macular CC (mean [SD] CC diameter, 9.3 [0.7] μm in the atrophic region vs 19.5 [0.9] μm in the nonatrophic region).

Grade 5

Neovascular disease was observed in 13 eyes, ranging from active or “viable” CNV (UEA⁺) to CNV within a disciform scar. A representative eye is shown in Figure 5 (patient 23, eTable in the Supplement). This patient was followed up for 16 years, initially graded 3A (visual acuity, 20/20), and later developed NV. This eye was treated with 6 anti-vascular endothelial growth factor (VEGF) injections.

Macular drusen, RPE detachment, and early atrophic changes subsequent to anti-VEGF treatment are apparent in infrared and spectral-domain OCT images (Figure 5A and B) obtained 0.8 years before death. The OCT did not show intraretinal or subretinal fluid. The original CNV is obvious in a fluorescein angiogram taken 4 years prior to the OCT and prior to treatment (Figure 5C). Although the most recent spectral-domain OCT images did not show active CNV requiring treatment, CNV was seen histopathologically (Figure 5D-G). Low-magnification imaging shows an active CNV membrane radiating from central feeder vessels, covering a submacular area of 5.8 mm². At the edge of the CNV, severe attenuation of the CC is apparent (Figure 5D and E) in an area with RPE (data not shown). This attenuation becomes more apparent at higher magnification (Figure 5F). Intense labeling at the edge of the CNV is apparent, representing hyperplastic endothelial cells. Outside the affected area, the CC has a few missing capillary segments, but the network is relatively normal (Figure 5G). The mean (SD) %VA immediately adjacent to CNV was 57.8% (3.6%) and the mean (SD) capillary diameter was 14.1 (0.4) μm.

Quantification of Choroidal Vasculature

The mean %VAs and CC diameters of a subset of eyes from each AMD group were compared with aged control participants (eFigure 3 in the Supplement). Because merged z-stacks were used for this image analysis, the density measurement included CC and intermediate blood vessels but not large vessels in the Haller layer. There were differences in mean %VA loss for comparisons of each AMD grade with control eyes. A 20.5% loss was observed in early AMD (95% CI, 11.2%-40.2%; $P < .001$); 12.5% loss in intermediate AMD (95% CI, 2.9%-21.4%; $P = .01$); 39.0% loss in GA (95% CI, 32.1%-45.4%; $P < .001$); and 38.2% loss adjacent to CNV (95% CI, 27.7%-47.9%; $P < .001$). The mean CC diameter among patients with GA was 29.6% lower compared with control individuals (mean difference, 4.3 μm; 95% CI, 2.8-5.9; $P < .001$, eFigure 3 in the Supplement). Submacular CC diameters did not differ between controls and other AMD groups.

Discussion

A role for CC dysfunction in AMD onset and progression has been suggested by our prior studies using alkaline phosphatase labeling^{6,12} and by other reports measuring a decrease in subfoveal blood flow with increasing AMD severity.¹³⁻¹⁵ Fluorescein angiography provides some insights into the pathophysiology of GA and NV but not for CC changes observed earlier in the AMD process. To our knowledge, this study is the first large case series evaluating extensive phenotypic data in conjunction with histopathologic analyses of the CC in all stages of AMD. Our results suggest that clinical observations of AMD underestimate both CC loss and involvement of the choroidal vasculature.

This study presents several important observations about CC changes. Ulex europaeus agglutinin staining suggests that RPE atrophy precedes CC loss in GA, while loss occurs in the absence of RPE atrophy in early AMD. Apparent neovascular buds were observed adjacent to areas of CC attenuation, and this hypercellularity may be the earliest form of NV. Choriocapillaris loss was also observed around large CNV formations and was associated with apparent buds and CNV formations in the presence of the RPE. We therefore hypothesize that RPE becomes hypoxic and may produce VEGF to fuel early and late CC endothelial cell proliferation prior to RPE atrophy. However, definitive conclusions regarding the proposed progression cannot be determined because this study was cross-sectional and evaluated a number of eyes.

Severe attenuation of the CC was more apparent in later AMD stages. We observed extensive submacular CC loss in eyes with both GA and NV. Results demonstrate that CC loss precedes RPE atrophy in eyes with NV, which is consistent with our previous findings.^{5,6} Participants with NV presented with severe CC attenuation in adjacent areas extending well beyond the border of the submacular CNV (> 1 mm). This study also reaffirms our previous observation that RPE death occurs prior to CC atrophy in GA.^{6,12} Different etiologies are therefore suggested for NV and GA: CC dies before RPE in NV, suggesting a vascular etiology; or CC dies secondary to RPE loss in GA when CC endothelial cells no longer have their constitutive source of VEGF, the RPE.^{16,17}

If vascular changes are indeed the initiating event in NV, this would be consistent with the known vascular risk profile for AMD. Body mass index, cigarette smoking, and nutritional intake are well-documented factors associated with AMD,^{2,18–21} particularly in relation to disease progression. Our predictive models have demonstrated the usefulness of these modifiable factors in assessing the transition to GA and NV.^{22–25} It is possible that their predictive capacity might be enhanced by incorporating structural changes in the choroidal vasculature as determined by OCT angiography (OCTA).

Submacular blood flow in CC decreases with age and further decreases in AMD.^{7,14,15,26} The use of OCTA has gained popularity because it allows for a noninvasive visualization of retinal and choroidal blood flow. This modality is being used to obtain high-resolution imaging that is superior to fluorescein angiography for many parameters.^{27,28} The ability to evaluate CC changes prior to any phenotypic change in the outer retinal layers or RPE suggests that OCTA could predict the onset of clinically diagnosed NV much earlier than with other imaging modalities.^{29–31} If our hypothesis is correct and localized CC dropout is a precursor to clinically apparent CNVs, OCTA could potentially identify this CC alteration in vivo, making “prophylactic” anti-VEGF therapy a treatment option to investigate for high-risk patients.

Our study is strengthened by a well-characterized and longstanding clinical cohort of patients with and without AMD. This unique resource allowed for comparisons between histopathology and a wealth of clinical data. Our results suggest that clinical observations underestimate the loss of CC and the involvement of the choroidal vasculature in AMD. Ulex europaeus agglutinin lectin labeling provides a robust marker for viable CC, and this method provided the first insights into CC changes in early and intermediate AMD. Our

study is limited by the number of available eyes. The mean age of the control group, despite the small sample size, was comparable to the mean age of patients with AMD. A larger cohort of control individuals and patients with early AMD is required to definitively determine whether CC loss is attributable to early AMD or to aging.

Conclusions

Extensive CC loss was observed in GA and NV. It is visible in early and intermediate stages, and the attenuation of CC progresses with the severity of AMD. As OCTA technology evolves, early CC loss may become a useful biomarker. Additional studies are required to further explore the pathophysiology underlying the early forms of AMD. Such research could shed light on preventive and therapeutic strategies prior to the observed onset of advanced disease.

Supplementary Material

Refer to Web version on PubMed Central for supplementary material.

Acknowledgments

Funding/Support: This research was supported by National Institutes of Health grants EY016151 (Dr Luty), EY01765 (Wilmer), and EY011309 (Dr Seddon); Arnold and Mabel Beckman Foundation (Drs Luty and Seddon); a Research to Prevent Blindness unrestricted grant; and the Macular Degeneration Research Fund, Tufts Medical Center and Tufts University School of Medicine, Boston, Massachusetts (Dr Seddon).

Role of the Funder/Sponsor: The funding sources had no role in the design and conduct of the study; collection, management, analysis, and interpretation of the data; preparation, review, or approval of the manuscript; and decision to submit the manuscript for publication.

References

1. Friedman DS, O'Colmain BJ, Muñoz B, et al. Eye Diseases Prevalence Research Group. Prevalence of age-related macular degeneration in the United States. *Arch Ophthalmol*. 2004; 122(4):564–572. [PubMed: 15078675]
2. Sobrin L, Seddon JM. Nature and nurture—genes and environment—predict onset and progression of macular degeneration. *Prog Retin Eye Res*. 2014; 40:1–15. [PubMed: 24374240]
3. Fritsche LG, Chen W, Schu M, et al. AMD Gene Consortium. Seven new loci associated with age-related macular degeneration. *Nat Genet*. 2013; 45(4):433–439. e1–e2. [PubMed: 23455636]
4. Lim LS, Mitchell P, Seddon JM, Holz FG, Wong TY. Age-related macular degeneration. *Lancet*. 2012; 379(9827):1728–1738. [PubMed: 22559899]
5. McLeod DS, Taomoto M, Otsuji T, Green WR, Sunness JS, Luty GA. Quantifying changes in RPE and choroidal vasculature in eyes with age-related macular degeneration. *Invest Ophthalmol Vis Sci*. 2002; 43(6):1986–1993. [PubMed: 12037009]
6. McLeod DS, Grebe R, Bhutto I, Merges C, Baba T, Luty GA. Relationship between RPE and choriocapillaris in age-related macular degeneration. *Invest Ophthalmol Vis Sci*. 2009; 50(10): 4982–4991. [PubMed: 19357355]
7. Bhutto I, Luty G. Understanding age-related macular degeneration (AMD): relationships between the photoreceptor/retinal pigment epithelium/Bruch's membrane/choriocapillaris complex. *Mol Aspects Med*. 2012; 33(4):295–317. [PubMed: 22542780]
8. Biesemeier A, Taubitz T, Julien S, Yoeruek E, Schraermeyer U. Choriocapillaris breakdown precedes retinal degeneration in age-related macular degeneration. *Neurobiol Aging*. 2014; 35(11): 2562–2573. [PubMed: 24925811]

9. Seddon JM, Sharma S, Adelman RA. Evaluation of the clinical age-related maculopathy staging system. *Ophthalmology*. 2006; 113(2):260–266. [PubMed: 16458093]
10. Edwards MM, McLeod DS, Bhutto IA, Villalonga MB, Seddon JM, Luty GA. Idiopathic preretinal glia in aging and age-related macular degeneration. *Exp Eye Res*. 2015; (15):S0014-4835. 00242-0.
11. Mullins RF, Johnson MN, Faidley EA, Skeie JM, Huang J. Choriocapillaris vascular dropout related to density of drusen in human eyes with early age-related macular degeneration. *Invest Ophthalmol Vis Sci*. 2011; 52(3):1606–1612. [PubMed: 21398287]
12. McLeod DS, Taomoto M, Otsuji T, Green WR, Sunness JS, Luty GA. Quantifying changes in RPE and choroidal vasculature in eyes with age-related macular degeneration. *Invest Ophthalmol Vis Sci*. 2002; 43(6):1986–1993. [PubMed: 12037009]
13. Grunwald JE, Hariprasad SM, DuPont J, et al. Foveolar choroidal blood flow in age-related macular degeneration. *Invest Ophthalmol Vis Sci*. 1998; 39(2):385–390. [PubMed: 9477998]
14. Grunwald JE, Metelitsina TI, Dupont JC, Ying GS, Maguire MG. Reduced foveolar choroidal blood flow in eyes with increasing AMD severity. *Invest Ophthalmol Vis Sci*. 2005; 46(3):1033–1038. [PubMed: 15728562]
15. Metelitsina TI, Grunwald JE, DuPont JC, Ying GS, Brucker AJ, Dunaief JL. Foveolar choroidal circulation and choroidal neovascularization in age-related macular degeneration. *Invest Ophthalmol Vis Sci*. 2008; 49(1):358–363. [PubMed: 18172113]
16. Marneros AG, Fan J, Yokoyama Y, et al. Vascular endothelial growth factor expression in the retinal pigment epithelium is essential for choriocapillaris development and visual function. *Am J Pathol*. 2005; 167(5):1451–1459. [PubMed: 16251428]
17. Saint-Geniez M, Maldonado AE, D'Amore PA. VEGF expression and receptor activation in the choroid during development and in the adult. *Invest Ophthalmol Vis Sci*. 2006; 47(7):3135–3142. [PubMed: 16799060]
18. Seddon JM, Willett WC, Speizer FE, Hankinson SE. A prospective study of cigarette smoking and age-related macular degeneration in women. *JAMA*. 1996; 276(14):1141–1146. [PubMed: 8827966]
19. Seddon JM, Ajani UA, Sperduto RD, et al. Eye Disease Case-Control Study Group. Dietary carotenoids, vitamins A, C, and E, and advanced age-related macular degeneration. *JAMA*. 1994; 272(18):1413–1420. [PubMed: 7933422]
20. Seddon JM, Rosner B, Sperduto RD, et al. Dietary fat and risk for advanced age-related macular degeneration. *Arch Ophthalmol*. 2001; 119(8):1191–1199. [PubMed: 11483088]
21. Reynolds R, Rosner B, Seddon JM. Dietary omega-3 fatty acids, other fat intake, genetic susceptibility, and progression to incident geographic atrophy. *Ophthalmology*. 2013; 120(5):1020–1028. [PubMed: 23481534]
22. Seddon JM, George S, Rosner B, Klein ML. CFH gene variant, Y402H, and smoking, body mass index, environmental associations with advanced age-related macular degeneration. *Hum Hered*. 2006; 61(3):157–165. [PubMed: 16816528]
23. Seddon JM, Reynolds R, Maller J, Fagerness JA, Daly MJ, Rosner B. Prediction model for prevalence and incidence of advanced age-related macular degeneration based on genetic, demographic, and environmental variables. *Invest Ophthalmol Vis Sci*. 2009; 50(5):2044–2053. [PubMed: 19117936]
24. Seddon JM, Reynolds R, Yu Y, Daly MJ, Rosner B. Risk models for progression to advanced age-related macular degeneration using demographic, environmental, genetic, and ocular factors. *Ophthalmology*. 2011; 118(11):2203–2211. [PubMed: 21959373]
25. Seddon JM, Silver RE, Kwong M, Rosner B. Risk prediction for progression of macular degeneration: 10 common and rare genetic variants, demographic, environmental, and macular covariates. *Invest Ophthalmol Vis Sci*. 2015; 56(4):2192–2202. [PubMed: 25655794]
26. Luty G, Grunwald J, Majji AB, Uyama M, Yoneya S. Changes in choriocapillaris and retinal pigment epithelium in age-related macular degeneration. *Mol Vis*. 1999; 5:35. [PubMed: 10562659]

27. de Carlo TE, Salz DA, Waheed NK, Bauman CR, Duker JS, Witkin AJ. Visualization of the retinal vasculature using wide-field montage optical coherence tomography angiography. *Ophthalmic Surg Lasers Imaging Retina*. 2015; 46(6):611–616. [PubMed: 26172062]
28. Ferrara D, Waheed NK, Duker JS. Investigating the choriocapillaris and choroidal vasculature with new optical coherence tomography technologies. *Prog Retin Eye Res*. 2016; 52:130–155. [PubMed: 26478514]
29. Jia Y, Bailey ST, Hwang TS, et al. Quantitative optical coherence tomography angiography of vascular abnormalities in the living human eye. *Proc Natl Acad Sci U S A*. 2015; 112(18):E2395–E2402. [PubMed: 25897021]
30. Schwartz DM, Fingler J, Kim DY, et al. Phase-variance optical coherence tomography: a technique for noninvasive angiography. *Ophthalmology*. 2014; 121(1):180–187. [PubMed: 24156929]
31. Lane M, Ferrara D, Louzada RN, Fujimoto JG, Seddon JM. Diagnosis and follow-up of nonexudative choroidal neovascularization with multiple optical coherence tomography angiography devices: a case report. *Ophthalmic Surg Lasers Imaging Retina*. 2016; 47(8):778–781. [PubMed: 27548457]

Key Points

Question

In a few eyes obtained post mortem, how severe was choriocapillaris loss among various stages of age-related macular degeneration (AMD), and when did it occur in relation to retinal pigment epithelial atrophy?

Findings

Choriocapillaris vascular area loss compared with 4 control individuals was 20.5% in early AMD, 12.5% in intermediate AMD, 39% in geographic atrophy, and 38.2% in neovascular AMD. Hypercellular buds suggestive of neovascularization were adjacent to choriocapillaris loss in 22.2% of early and 40% of intermediate AMD eyes.

Meaning

While based on a small number of eyes, these findings suggest choriocapillaris loss occurs during early and intermediate AMD and increases with progression to advanced disease.

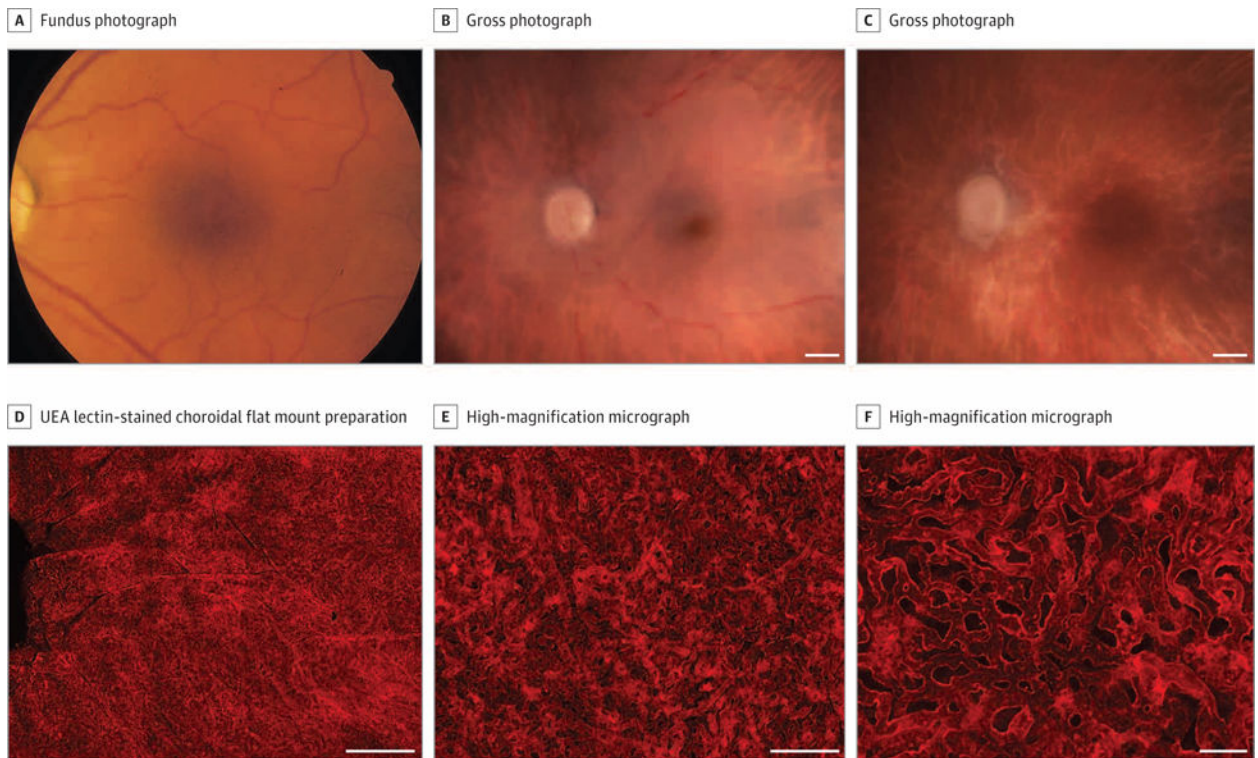


Figure 1. Grade 1, Patient 3, Left Eye

Fundus photograph (A), gross photographs (B-C), and Ulex europaeus agglutinin (UEA) lectin-stained choroidal flat mount preparation (D-F) from an 87-year-old white woman with no history of age-related macular degeneration. The fundus photograph (A) shows a normal appearance of the macula. Postmortem gross photographs of the posterior eyecup with the retina intact (B) and the retina removed (C) show absence of drusen, retinal pigment epithelium loss, or hyperpigmentation. Low-magnification confocal micrograph of the UEA choroidal flat mount shows normal homogeneous pattern of choriocapillaris in the posterior pole region (D). Higher-magnification micrographs (E-F) show broad-diameter freely interconnecting capillaries. The mean (SD) percent vascular area in the submacula was 77.8% (3.5%) and the mean (SD) choriocapillaris diameter was 12.8 (1.2) μm . Scale bars: B-D = 1 mm, E = 200 μm ; F = 50 μm .

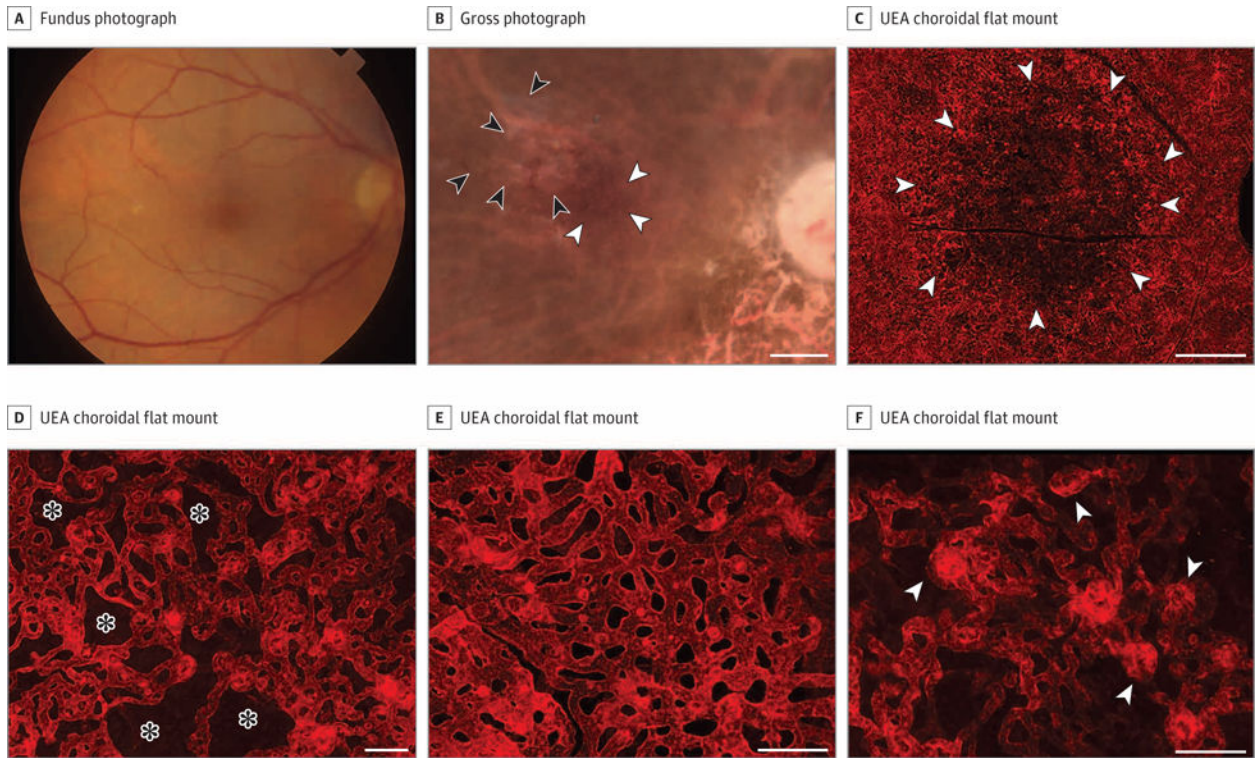


Figure 2. Grade 2C, Patient 10, Right Eye

Fundus photograph (A), gross photograph (B), and *Ulex europaeus* agglutinin (UEA) lectin-stained choroidal flat mount preparation (C-F) from an 86-year-old white woman with a history of early-stage AMD. The fundus photograph (A) shows drusen in the macula. Postmortem gross photograph with the retina removed (B) shows presence of drusen (black arrowheads) and some pigmentary abnormalities (white arrowheads). Low-magnification confocal micrograph of the UEA choroidal flat mount shows a region of choriocapillaris (CC) pathology (arrowheads) in the submacula that was 10.5 mm² (C). Higher-magnification micrographs show loss of interconnecting capillary channels (asterisks) and thinning of the CC lumen in submacula (D) compared with broad-diameter freely interconnecting capillaries in the perimacular region (E). At the border of submacular CC atrophy, small apparent neovascular buds (arrowheads) were observed (F). The mean (SD) percent vascular area was 43% (8.7%) in the submacula compared with 76% (2.8%) in the perimacular region. The mean (SD) CC diameter was 13.5 (0.7) μ m in the submacular region compared to 17.4 (1.8) μ m in the perimacular region. Scale bars: B and C = 1 mm, D-F = 50 μ m.

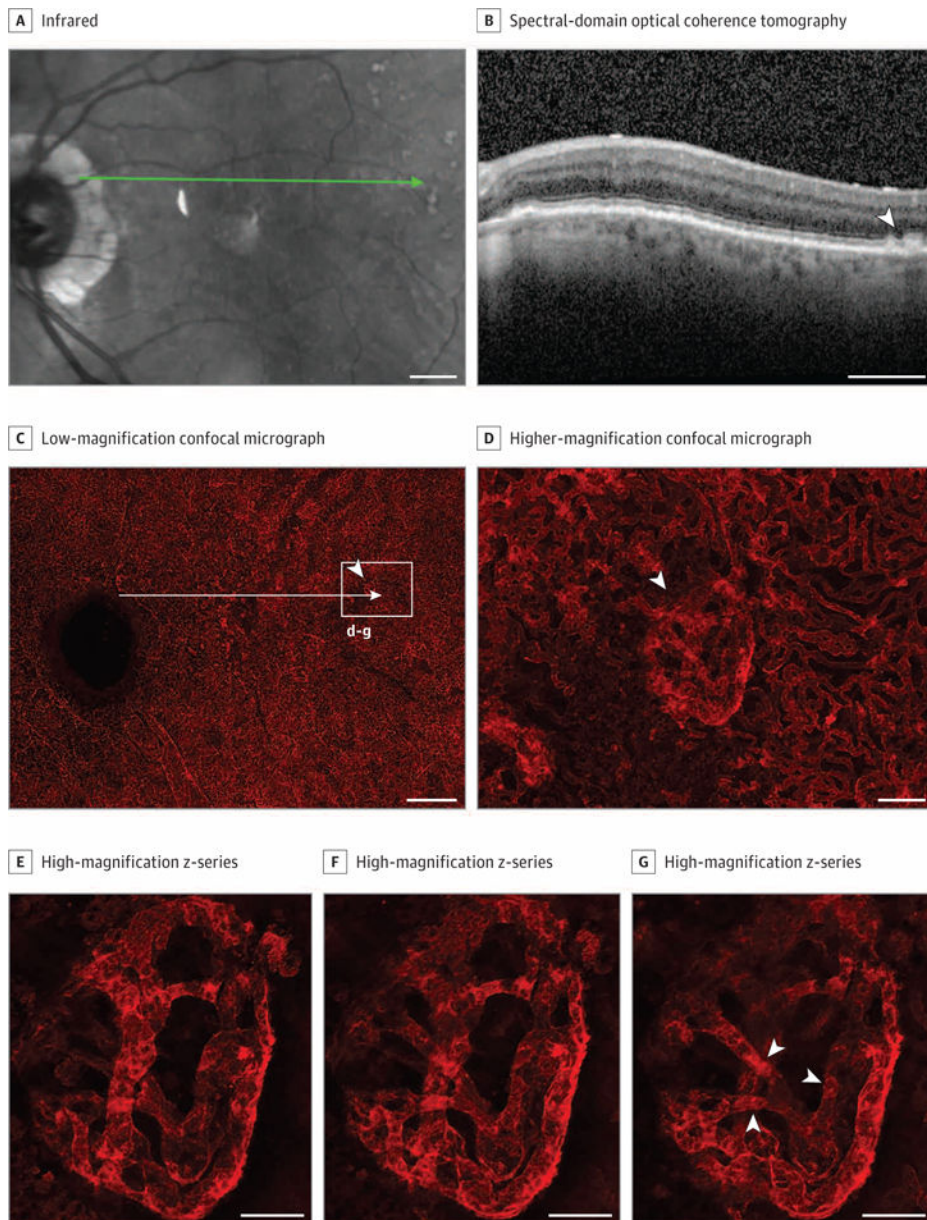


Figure 3. Grade 3, Patient 13, Left Eye

Infrared image (A) and spectral-domain optical coherence tomography (OCT) (B) obtained 3 months prior to death, and Ulex europaeus agglutinin (UEA) lectin-stained choroidal flat mount preparation (C-G) from a 93-year-old white man with a history of intermediate AMD (grade 3). The infrared image shows numerous drusen in the posterior pole with some apparent pigmentary abnormalities (A) in the macula and large drusen (arrowhead) on OCT (B). Low-magnification confocal micrograph of the UEA choroidal flat mount (C) shows reduced choriocapillaris density throughout submacula. The long arrow is an approximation of the position of the green scan line in A. Higher-magnification micrograph (D) of the region indicated by box in C shows loss of interconnecting capillary channels and a vascular malformation (arrowhead) that corresponds to the region indicated by the arrow in the OCT. High-magnification Z-series (E-G) of the vascular formation shown in D demonstrates that it

is internal to the choriocapillaris and represents a form of choroidal neovascularization. It has multiple connections to the underlying choroidal vasculature (arrowheads in G). Scale bars: A-C = 1 mm, D-F = 100 μ m.

Author Manuscript

Author Manuscript

Author Manuscript

Author Manuscript

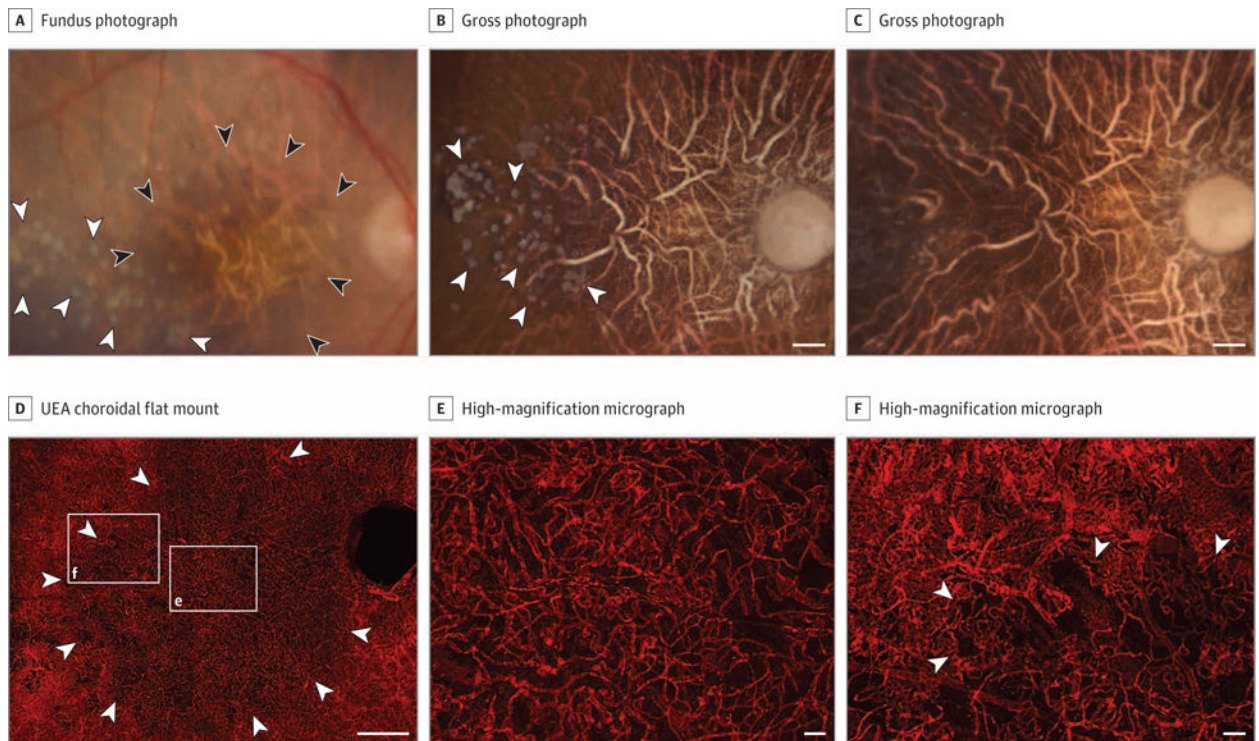


Figure 4. Grade 4, Patient 15, Right Eye

Fundus photograph (A), gross photographs (B and C), and Ulex europaeus agglutinin (UEA) lectin-stained choroidal flat mount preparation (D-F) from a 97-year-old white woman with a history of geographic atrophy. The fundus photograph (A) shows a well-defined area of retinal pigment epithelial (RPE) atrophy in the macula (black arrowheads) and drusen adjacent to the region of atrophy (white arrowheads). Postmortem gross photograph of the posterior eyecup with the retina removed prior to EDTA treatment (B) shows presence of glistening white calcified drusen in the RPE layer (arrowheads). Gross photograph of the posterior eyecup following EDTA treatment to remove RPE (C) shows loss of calcified drusen. Low-magnification confocal micrograph of the UEA choroidal flat mount shows region of choriocapillaris (CC) pathology (arrowheads) in the posterior pole region corresponding to area of RPE atrophy that was 37.5 mm² (D). Higher-magnification micrographs show loss of interconnecting capillary channels and thinning of the CC lumen in the area of atrophy (box “e” in D) and at the border (arrowheads) of atrophy (box “f” in D). The mean (SD) percent vascular area was 38.3% (5%) in the area with RPE atrophy in the submacular region compared with 81.9% (23.9%) outside the area of RPE atrophy. The mean (SD) CC diameter was 9.3 (0.7) μm in the atrophic region compared with 19.5 (0.9) μm in the nonatrophic region. Scale bars: B-D = 1 mm, E and F = 50 μm.

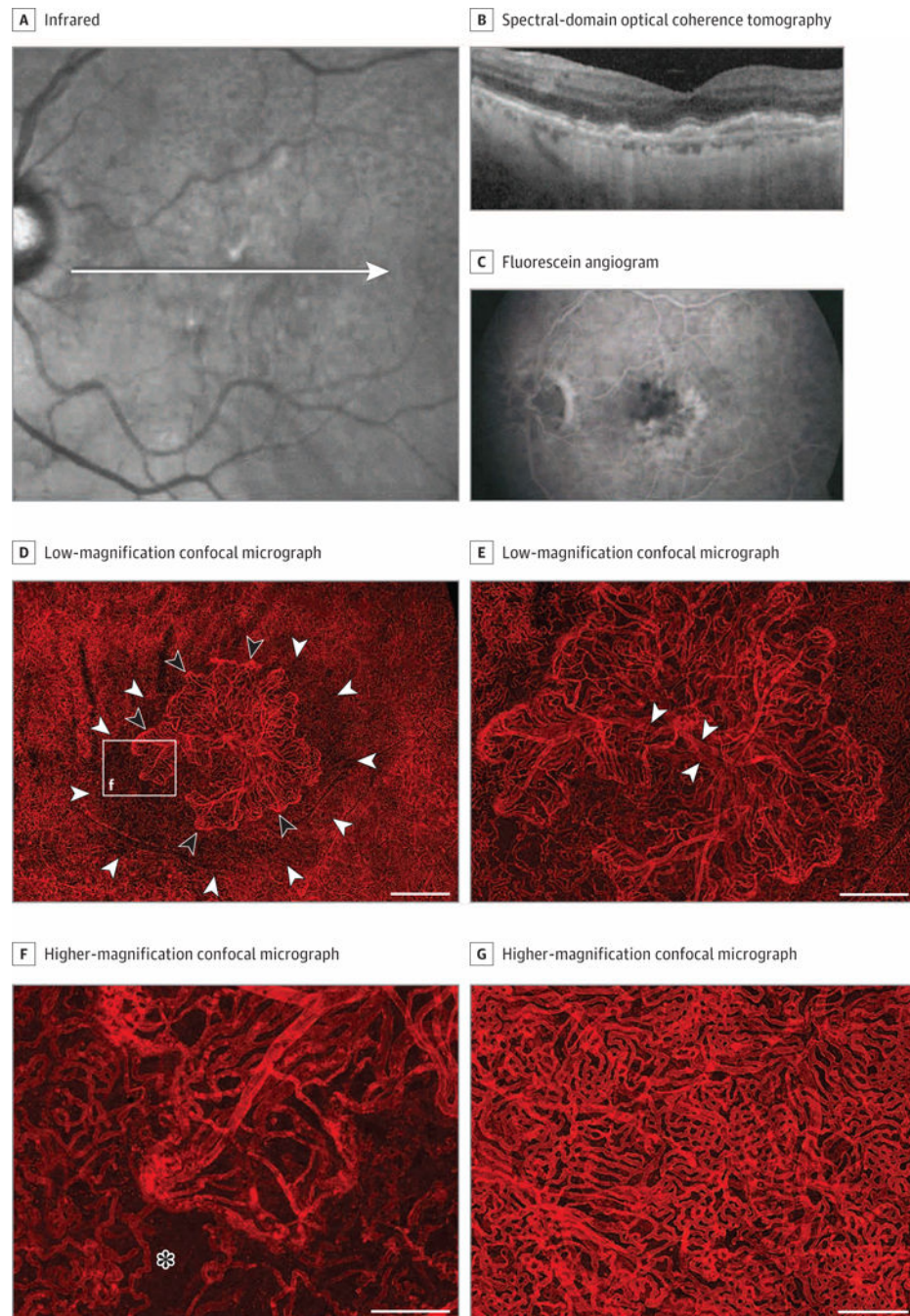


Figure 5. Grade 5, Patient 23, Left Eye

Infrared and spectral-domain optical coherence tomography (OCT) images (A and B), a fluorescein angiogram (C), and Ulex europaeus agglutinin (UEA) lectin-stained choroid (D-G) from an 84-year-old white man with a history of neovascular disease treated with 6 anti-vascular endothelial growth factor injections. The infrared and OCT images (A and B) show drusen (including reticular-type drusen), retinal pigment epithelial (RPE) detachment, and early atrophic changes. The fluorescein angiogram prior to treatment displays the active choroidal neovascularization (CNV) (C). Low-magnification confocal micrograph of the

UEA choroidal flat mount shows a CNV formation (black arrowheads) in the submacula, which was 5.8 mm² (D and E). Choriocapillaris attenuation extended well beyond the edge of the CNV (white arrowheads in D). Higher-magnification micrograph (F) shows edge of CNV (area in box “f” in D) with looped hypercellular tips of neovascular vessels and capillary dropout adjacent to the edge of the CNV (asterisk). Peripheral to the CNV (G), the choriocapillaris has normal morphology. Scale bars: D = 1 mm, E = 500 μm, F and G = 250 μm.

Author Manuscript

Author Manuscript

Author Manuscript

Author Manuscript